Thin-Stratified Medium Fast-Multipole Algorithm for Solving Microstrip Structures

Jun-Sheng Zhao, Weng Cho Chew, *Fellow, IEEE,* Cai-Cheng Lu, *Member, IEEE,* Eric Michielssen, *Member, IEEE,* and Jiming Song, *Member, IEEE*

***Abstract*—An accurate and efficient technique called the thin-stratified medium fast-multipole algorithm (TSM-FMA) is presented for solving integral equations pertinent to electromagnetic analysis of microstrip structures, which consists of the full-wave analysis method and the application of the multilevel fast multipole algorithm (MLFMA) to thin stratified structures. In this approach, a new form of the electric-field spatial-domain Green's function is developed in a symmetrical form which simplifies the discretization of the integral equation using the method of moments (MoM). The patch may be of arbitrary shape since their equivalent electric currents are modeled with subdomain triangular patch basis functions. TSM-FMA is introduced to speed up the matrix–vector multiplication which constitutes the major computational cost in the application of the conjugate gradient (CG) method. TSM-FMA reduces the central processing unit (CPU) time per iteration to $O(N \log N)$ for sparse structures and to $O(N)$ for dense structures, from $O(N^3)$ for the Gaussian elimination method and $O(N^2)$ per iteration for the CG method. The memory requirement for TSM-FMA also scales as $O(N \log N)$ for sparse structures and as $O(N)$ for dense structures. Therefore, this approach is suitable for solving large-scale problems on a small computer.**

***Index Terms*— Fast multipole, integral equation, method of moments, microstrip, multilevel algorithm.**

I. Introduction

MICROSTRIP structures have been studied extensively using various types of full-wave analysis techniques. However, these techniques are still fraught with difficulties because they usually involve the solution of a very large system of linear equations. Some authors have analyzed large microstrip antenna arrays composed of uniform elements as infinitely large arrays based on a Floquet-type representation of fields. However, the simplifying assumptions used in this technique render it incapable of dealing with spurious radiation from the network, edge effects, and irregular structures. The spectral-domain conjugate gradient fast Fourier transform (CG-FFT) method [1] can be used to solve large microstrip problems. However, a large amount of padding of the FFT is required to reduce aliasing errors because of the slow rate of decay of the Green's function in the spectral domain. To solve this problem, the spatial-domain CG-FFT, which applies the CG-FFT method in conjunction with the complex discrete image technique, has been proposed [2], but for sparse structures, this method is not very efficient because many unnecessary interstitial zero paddings are introduced. The complex discrete image technique has also been used in conjunction with the fast multipole method (FMM) [3], [4].

The multilevel fast multipole algorithm (MLFMA) [5], [6] speeds up the solution of the linear equations and reduces the memory requirement. In this paper, the two-dimensional (2-D) MLFMA is introduced to solve the linear equations derived from the full-wave analysis method for microstrip structures. Here, 2-D MLFMA is the adaptation of the FMM for the Helmholtz equation [7] first proposed for acoustic waves and the multilevel algorithm involving interpolation and anterpolation [8].

This proposed method is most efficient when the transverse dimension of the microstrip structure is much larger than its vertical dimension. Hence, we shall term the proposed technique the thin-stratified medium fast-multipole algorithm (TSM-FMA). Here, a three-dimensional (3-D) problem is numerically approximated by a quasi-2-D problem by the use of the steepest descent path integration [9]–[12] before MLFMA is applied. The method is exact in as far as numerical computation is concerned (since the accuracy can be controlled), although it is most efficient for the microstrip structures.

Furthermore, in this approach, a new symmetrical form of electric-field spatial-domain Green's function different from [13] and [14] is introduced. When the method of moments (MoM) is used to discretize the integral equation, the differential operators appearing in the Green's function are moved from the singular Green's function onto the differentiable basis and testing functions. As a result, the remaining parts of the Green's function are less singular. The electric-field dyadic Green's function entails Sommerfeld-type integrals whose highly oscillatory and slowly converging behavior of the integrands renders their numerical evaluation difficult. To accelerate the calculation of these Green's functions, the Fourier inversion contour is deformed to the vertical branch cut (which is also the steepest descent path [15]) when the thickness of the substrate is small compared to its transverse

Manuscript received June 17, 1997; revised October 13, 1997. This work was supported by Air Force Office of Scientific Research under MURI Grant F49620-96-1-0025, by the Office of Naval Research under Grant N00014-95-1-0872, and by the National Science Foundation (NSF) under Grant NSF ECS93-02145.

J.-S. Zhao, W. C. Chew, and E. Michielssen are with the Center for Computational Electromagnetics, Electromagnetics Laboratory, Department of Electrical and Computer Engineering, University of Illinois, Urbana, IL 61801 USA.

C.-C. Lu is with Demaco, Inc., Champaign, IL 61820 USA.

J. Song is with the Center for Computational Electromagnetics, Electromagnetics Laboratory, Department of Electrical and Computer Engineering, University of Illinois Urbana, IL 61801 USA, and with Demaco, Inc., Champaign, IL 61820 USA.

Publisher Item Identifier S 0018-9480(98)02730-6.

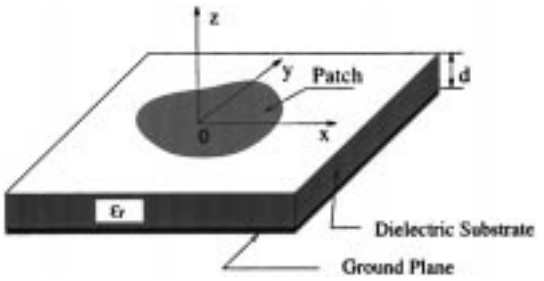

Fig. 1. Geometry of microstrip structure.

dimension. This is true for most microstrip structures. This contour deformation allows a very efficient representation of the layered-medium Green's function by a small summation of 2-D Green's functions, casting it into a quasi-2-D problem.

The subdomain triangular patch basis function is used to model equivalent electric currents on the patch, so that the patch may be of an arbitrary shape. To solve the matrix equation, conjugate gradient (CG) methods are preferred over direct methods. The major computational cost in CG lies in the matrix–vector multiplication.

TSM-FMA reduces the central processing unit (CPU) time per iteration to $O(N \log N)$ for sparse structures and to $O(N)$ for dense structures, from $O(N^3)$ for the Gaussian elimination method and $O(N^2)$ per iteration for the CG method, where N is the number of unknowns. The memory requirement for TSM-FMA is also $O(N \log N)$ for sparse structures and $O(N)$ for dense structures. It has to be emphasized that the reduction in computational complexity is not at the expense of numerical precision—the precision of this method can be controlled to any desired accuracy. Therefore, the proposed approach is suitable for solving large problems on a small computer.

II. Formulation

The general geometry of a microstrip structure is shown in Fig. 1. The substrate is assumed to be infinite in the xy-plane, and the metallized patches are assumed to be perfectly conducting and infinitesimally thin. For simplicity, conductor and substrate losses are neglected, but the thin substrate can be multilayered.

An electric-field integral equation (EFIE) can be constructed by enforcing the total electric-field tangential to the surface S to vanish

$$\hat{z} \times \int_S \overline{\boldsymbol{G}}(\boldsymbol{r}, \boldsymbol{r}') \cdot \boldsymbol{J}(\boldsymbol{r}')\, dS' = -\hat{z} \times \boldsymbol{E}^{\text{inc}}(\boldsymbol{r}) \tag{1}$$

where $\overline{\boldsymbol{G}}$ is the dyadic electric-field Green's function, and $\boldsymbol{J}$ is the surface-current distribution. The prime represents the variables or operators associated with sources. The excitation field $\boldsymbol{E}^{\text{inc}}(\boldsymbol{r})$ can be the field of a impinging plane wave or the field created by a finite source residing within the microstrip structure.

A. Dyadic Green's Function

Before discretizing the EFIE (1), equations for the dyadic Green's function are presented. The spectral-domain Green's function can be derived in a closed form. It can be written as the sum of TE and TM to z-waves propagating in the $+z$- and $-z$-direction due to reflection and transmission at the stratified medium interfaces. Using the (E_z, H_z) formulation [15], [16], after some derivations, the spectral-domain dyadic Green's function $\tilde{\overline{\boldsymbol{G}}}$ in the region $z \geq 0$ can be written in a symmetric form as follows:

$$\begin{aligned}\hat{\alpha} \cdot \tilde{\overline{\boldsymbol{G}}} \cdot \hat{\alpha}' = {} & (\hat{\alpha}_s \cdot \hat{\alpha}_s')(\tilde{g}^p - \tilde{g}^{\text{TE},R}) + \alpha_z \alpha_z' (\tilde{g}^p + \tilde{g}^{\text{TM},R}) \\ & + \frac{1}{k^2}\, \hat{\alpha} \cdot \nabla\nabla \cdot \hat{\alpha}' \tilde{g}^p + \frac{1}{k^2}\, \hat{\alpha} \cdot \nabla\nabla \cdot \tilde{\hat{\alpha}}' \tilde{g}^{\text{TM},R} \\ & + \hat{\alpha} \cdot \nabla_s \nabla_s \cdot \tilde{\hat{\alpha}}' \tilde{g}^{\text{EM}}\end{aligned} \tag{2}$$

where

$$\begin{aligned}\hat{\alpha} &= \hat{\alpha}_s + \alpha_z \hat{z} \\ \hat{\alpha}' &= \hat{\alpha}_s' + \alpha_z' \hat{z} \\ \tilde{\hat{\alpha}}' &= -\hat{\alpha}_s' + \alpha_z' \hat{z} \\ \tilde{g}^{\text{EM}} &= \frac{1}{k_s^2}\, (\tilde{g}^{\text{TE},R} - \tilde{g}^{\text{TM},R}) \\ \tilde{g}^p &= -\frac{\omega\mu_0}{8\pi^2}\, \frac{e^{i\boldsymbol{k}_s \cdot (\boldsymbol{r}_s - \boldsymbol{r}_s')}}{k_z}\, e^{ik_z |z - z'|} \\ \tilde{g}^{\text{TM},R} &= -\frac{\omega\mu_0}{8\pi^2}\, \tilde{R}^{\text{TM}}\, \frac{1}{k_z}\, e^{i\boldsymbol{k}_s \cdot (\boldsymbol{r}_s - \boldsymbol{r}_s')} e^{ik_z (z + z')} \\ \tilde{g}^{\text{TE},R} &= \frac{\omega\mu_0}{8\pi^2}\, \tilde{R}^{\text{TE}}\, \frac{1}{k_z}\, e^{i\boldsymbol{k}_s \cdot (\boldsymbol{r}_s - \boldsymbol{r}_s')} e^{ik_z (z + z')} \\ k_z &= \sqrt{k^2 - k_s^2}\end{aligned}$$

k is the wavenumber in free space, $k_s^2 = k_x^2 + k_y^2 = k_\rho^2$, and $\tilde{R}^{\text{TE,TM}}$ is the generalized reflection coefficient for the layered medium.

The spectral integration of (2) yields the spatial-domain Green's function as follows:

$$\begin{aligned}\hat{\alpha} \cdot \overline{\boldsymbol{G}} \cdot \hat{\alpha}' = {} & (\hat{\alpha}_s \cdot \hat{\alpha}_s')(g^p - g^{\text{TE},R}) + \alpha_z \alpha_z' (g^p + g^{\text{TM},R}) \\ & + \frac{1}{k^2}\, \hat{\alpha} \cdot \nabla\nabla \cdot \hat{\alpha}' g^p + \frac{1}{k^2}\, \hat{\alpha} \cdot \nabla\nabla \cdot \tilde{\hat{\alpha}}'\, g^{\text{TM},R} \\ & + \hat{\alpha} \cdot \nabla_s \nabla_s \cdot \tilde{\hat{\alpha}}'\, g^{\text{EM}}\end{aligned} \tag{3}$$

where

$$\begin{aligned} g^\beta &= \int_{-\infty}^{+\infty} \int_{-\infty}^{+\infty} \tilde{g}^\beta\, dk_x\, dk_y \\ \beta &= p, (\text{TE}, R), (\text{TM}, R), \text{EM}. \end{aligned}$$

To convert the spectral-domain Green's function into the spatial-domain Green's function, twofold integrals are first reduced to onefold integrals by coordinate system transform from Cartesian to polar. Since Sommerfeld-type integrals are involved, their evaluation is very time consuming since the integrands are both highly oscillatory and slowly decaying. To accelerate the evaluation of the Green's function, different techniques are used depending on the distance between the observation and source points.

First, for the case when the observation and source points overlap or are very close, the dominant factor that causes the time-consuming evaluation of the integrals is the singularity or near singularity of the integrands. To overcome this difficulty,

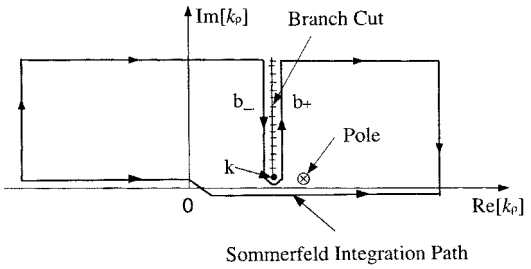

Fig. 2. Deformation of the Fourier inversion contour to the vertical branch cut.

the quasi-static terms are first extracted before the integrals are evaluated numerically. The quasi-static terms, corresponding to the asymptotic terms of the integrands, can be evaluated in closed forms by using the Sommerfeld identity. The remaining integrals, which converge fast, are computed along a contour deformed off the real axis in the k_ρ-plane to avoid the surface-wave pole.

Second, for the case when observation and source points are well separated, the original integration path in polar coordinates is first changed to the Sommerfeld integration path and then is deformed to the vertical branch cut [9], [10], as shown in Fig. 2. In the course of doing so, contributions from any pertinent pole singularities are included.

By a change of variable of $k_\rho = k + is$, and then $s = u^2$ to eliminate the singular term $1/\sqrt{s}$ appearing in the integrands and combining the integrations along the two sides of the vertical branch cut to simplify the integration, the terms needing evaluation in the Green's function can be rewritten as

$$g^p = -\frac{i\omega\mu_0}{2\pi}\int_0^{+\infty}\frac{(k+iu^2)}{\sqrt{2k+iu^2}e^{i(3\pi/4)}}H_0^{(1)}((k+iu^2)\rho)\,du \tag{4}$$

$$g^{\mathrm{TM},R} = -\frac{i\omega\mu_0}{4\pi}\int_0^{+\infty}\left(\tilde{R}_0^{\mathrm{TM}}+\frac{1}{\tilde{R}_0^{\mathrm{TM}}}\right)\cdot\frac{(k+iu^2)}{\sqrt{2k+iu^2}e^{i(3\pi/4)}}H_0^{(1)}((k+iu^2)\rho)\,du - \frac{i\omega\mu_0}{4}\,\mathrm{Res}\left[\tilde{R}^{\mathrm{TM}}\,\frac{k_\rho}{k_z}\,H_0^{(1)}(k_\rho\rho)\right] \tag{5}$$

$$g^{\mathrm{TE},R} = \frac{i\omega\mu_0}{4\pi}\int_0^{+\infty}\left(\tilde{R}_0^{\mathrm{TE}}+\frac{1}{\tilde{R}_0^{\mathrm{TE}}}\right)\cdot\frac{(k+iu^2)}{\sqrt{2k+iu^2}e^{i(3\pi/4)}}H_0^{(1)}((k+iu^2)\rho)\,du \tag{6}$$

$$g^{\mathrm{EM}} = \frac{i\omega\mu_0}{4\pi}\int_0^{+\infty}\left(\tilde{R}_0^{\mathrm{TE}}+\frac{1}{\tilde{R}_0^{\mathrm{TE}}}+\tilde{R}_0^{\mathrm{TM}}+\frac{1}{\tilde{R}_0^{\mathrm{TM}}}\right)\cdot\frac{1}{(k+iu^2)\sqrt{2k+iu^2}e^{i(3\pi/4)}}H_0^{(1)}((k+iu^2)\rho)\,du + \frac{i\omega\mu_0}{4}\,\mathrm{Res}\left[\tilde{R}^{\mathrm{TM}}\,\frac{1}{k_\rho k_z}\,H_0^{(1)}(k_\rho\rho)\right]. \tag{7}$$

The formulation up to this point is valid for arbitrary layered media. For the special case of a substrate backed by a ground plane

$$\tilde{R}_0^{\mathrm{TM}} = \frac{R_0^{\mathrm{TM}}+e^{2ik_{1z}d}}{1+R_0^{\mathrm{TM}}e^{2ik_{1z}d}}$$

$$R_0^{\mathrm{TM}} = \frac{\epsilon_r u\sqrt{2k+iu^2}e^{i(3\pi/4)}-k_{1z}}{\epsilon_r u\sqrt{2k+iu^2}e^{i(3\pi/4)}+k_{1z}}$$

$$\tilde{R}_0^{\mathrm{TE}} = \frac{R_0^{\mathrm{TE}}-e^{2ik_{1z}d}}{1-R_0^{\mathrm{TE}}e^{2ik_{1z}d}}$$

$$R_0^{\mathrm{TE}} = \frac{u\sqrt{2k+iu^2}e^{i(3\pi/4)}-k_{1z}}{u\sqrt{2k+iu^2}e^{i(3\pi/4)}+k_{1z}}$$

where $k_{1z}=\sqrt{k_1^2-(k+iu^2)^2}$. For thin-stratified media, the vertical branch cut is also the steepest descent path. Hence, integrations along this new path converge exponentially fast as a result of the exponential decay of the integrands for increasing s or u. The pole near the branch point of the TM term causes the integrand to vary rapidly near the pole. Hence, more points are needed within this range when using Gaussian quadrature to perform the integration. The integration range is first divided into two ranges, one of which is very close to the branch point. Then the integrations are performed over these two ranges using standard Gaussian–Legendre quadrature. For a fixed $\rho = |\boldsymbol{r}-\boldsymbol{r}'|$ range, only a few Gaussian integration points are needed to perform the integrations with good accuracy.

B. Discretizing the EFIE

MoM is applied to convert EFIE (1) into a linear algebraic system of equations. The first step is to expand the unknown current distribution in a set of basis functions

$$\boldsymbol{J}(\boldsymbol{r}) = \sum_{n=1}^{N} I_n \boldsymbol{J}_n(\boldsymbol{r}). \tag{8}$$

To model an arbitrarily shaped microstrip geometry, the vector triangular basis function defined by Rao, Wilton, and Glisson (RWG) [17] is adopted. This kind of basis function has been used extensively to model planar and nonplanar vector surface currents.

The Galerkin procedure is applied to create the matrix equation

$$\overline{Z}\cdot\boldsymbol{I} = \boldsymbol{V}. \tag{9}$$

After moving the differential operators from the singular Green's function onto the differentiable basis and testing functions by applying integration by parts, the matrix element can be expressed as

$$Z_{mn} = \int_{S_m} dS \int_{S_n'} dS'\,\boldsymbol{J}_m(\boldsymbol{r})\cdot\boldsymbol{J}_n(\boldsymbol{r}')(g^p - g^{\mathrm{TE},R}) - \int_{S_m} dS \int_{S_n'} dS'\nabla_s\cdot\boldsymbol{J}_m(\boldsymbol{r})\nabla_s' \cdot\boldsymbol{J}_n(\boldsymbol{r}')\left[\frac{1}{k^2}\,(g^p - g^{\mathrm{TM},R}) - g^{\mathrm{EM}}\right]. \tag{10}$$

The computation of the elements of $\boldsymbol{V}$ depends on the nature of the source. If the network parameters are desired, the impressed incident electric field $\boldsymbol{E}^{\text{inc}}$ can be chosen as the field generated by a series voltage gap source [18] placed across the edge associated with a single basis function. As a result, only one nonzero element exists in the excitation vector $\boldsymbol{V}$, and can be normalized to 1 V. The choice of the location of the voltage gap depends on the structure of the patches and the parameters to be calculated. For instance, if the input impedance of a side-fed microstrip antenna is desired, the voltage gap can be placed near the end of the microstrip line feeding the patch. Note, however, that a microstrip line of moderate length ($>\lambda/4$) is required to allow a dominant-mode incident wave to be generated. If the radar cross section (RCS) is desired, a unit amplitude plane wave of the form

$$\boldsymbol{E}_0^{\text{inc}} = \boldsymbol{E}_0 e^{i\boldsymbol{k}^{\text{inc}}\cdot\boldsymbol{r}}, \qquad |\boldsymbol{E}_0| = 1 \tag{11}$$

is assumed to excite the patch antenna, and a plane wave $\boldsymbol{E}^{\text{ref}}$ will be specularly reflected from the grounded dielectric slab, so that $\boldsymbol{E}^{\text{inc}} = \boldsymbol{E}_0^{\text{inc}} + \boldsymbol{E}^{\text{ref}}$ satisfies the appropriate boundary conditions at the air–dielectric interface and on the ground plane. The excitation elements are

$$V_m = -\int_S \boldsymbol{J}_m \cdot \boldsymbol{E}^{\text{inc}}\, dS, \qquad m = 1, 2, \cdots, N. \tag{12}$$

Applying reciprocity theorem to (12) leads to

$$V_m = -\frac{4\pi \boldsymbol{E}_m \cdot \boldsymbol{E}_o}{i\omega\mu_0} \tag{13}$$

where $4\pi/i\omega\mu_0$ is the required strength of an infinitesimal dipole source to produce a unit amplitude spherical wave e^{ikr}/r. Since it is necessary to evaluate the far-zone fields $\boldsymbol{E}_m$ $(m = 1, 2, \cdots, N)$ due to currents $\boldsymbol{J}_m$ in order to obtain the RCS, (13) uses less computational time compared to (12). The far-zone field when $z - z' > 0$ can be derived by using the stationary phase method [15], [19].

III. Thin-Stratified Medium Fast-Multipole Algorithm (TSM-FMA)

In solving the matrix equation (9), the CG method with $O(N^2)$ floating-point operations per iteration is preferred over direct methods which require $O(N^3)$ floating-point operations. The most costly part in a CG method is the matrix–vector multiplication. To speed up the matrix–vector multiplication, TSM-FMA (an adaptation of MLFMA [5], [6] to stratified medium Green's function) is used. After deforming the integration path from the Sommerfeld integration path to the vertical branch cut, the integration along the vertical branch cut can be performed in terms of only very few Gaussian integration points, resulting in the representation of the stratified medium Green's function by a sum of 2-D Green's functions. The efficiency of the matrix–vector multiplication is further enhanced by the adaptation of 2-D MLFMA.

To implement TSM-FMA, the entire patch is first enclosed in a large square, which is partitioned into four smaller squares. Each subsquare is then recursively subdivided into smaller squares until the smallest squares measure approximately $(0.25\lambda^2)$.

As discussed in Section II-A, when the observation and source points are well separated, the inverse transform of the Green's function can be performed with only a few Gaussian integration points along the vertical branch cut plus a pole contribution. By substituting the summation expression for the vertical branch-cut contribution of the Green's functions into (10), matrix elements describing interaction between basis and testing functions residing in well-separated groups can be written in the form below:

$$\begin{aligned} Z_{mn} = &\int_{S_m} dS \int_{S_n'} dS'\, \boldsymbol{J}_m(\boldsymbol{r}) \\ &\cdot \boldsymbol{J}_n(\boldsymbol{r}') \sum_j w_{1j}^u g^a(k_{uj}) H_0^{(1)}(k_{uj}|\boldsymbol{r} - \boldsymbol{r}'|) \\ &- \int_{S_m} dS \int_{S_n'} dS'\, \nabla_s \cdot \boldsymbol{J}_m(\boldsymbol{r}) \nabla_s' \\ &\cdot \boldsymbol{J}_n(\boldsymbol{r}') \sum_j w_{1j}^u g^q(k_{uj}) H_0^{(1)}(k_{uj}|\boldsymbol{r} - \boldsymbol{r}'|) \end{aligned} \tag{14}$$

where k_{uj} represents the pole and points along the vertical branch cut used in the integration. The above equation can be rewritten as follows by applying the 2-D MLFMA:

$$\begin{aligned} &Z_{mn} \\ &= \sum_j w_j^u g^a(k_{uj}) \frac{1}{2\pi} \int_0^{2\pi} d\alpha\, \tilde{\boldsymbol{\beta}}_{mk_{(1)}}^{aj}(\alpha) \cdot T_{k_{(1)}k_{(1)}'}^{j}(\alpha) \\ &\quad \cdot \tilde{\boldsymbol{\beta}}_{k_{(1)}'n}^{aj}(\alpha) - \sum_j w_j^u g^q(k_{uj}) \frac{1}{2\pi} \int_0^{2\pi} d\alpha \\ &\quad \cdot \tilde{\beta}_{mk_{(1)}}^{qj}(\alpha)\, T_{k_{(1)}k_{(1)}'}^{j}(\alpha) \tilde{\beta}_{k_{(1)}'n}^{qj}(\alpha) \end{aligned} \tag{15}$$

where

$$\begin{aligned} &\tilde{\boldsymbol{\beta}}_{mk_{(1)}}^{aj}(\alpha) \\ &\quad = \int_{S_m} dS\, \boldsymbol{J}_m(\boldsymbol{r}) e^{ik_{uj}\rho_{mk_{(1)}}\cos(\alpha + \phi_{mk_{(1)}})} \\ &\tilde{\beta}_{mk_{(1)}}^{qj}(\alpha) \\ &\quad = \int_{S_m} dS\, \nabla_s \cdot \boldsymbol{J}_m(\boldsymbol{r}) e^{ik_{uj}\rho_{mk_{(1)}}\cos(\alpha + \phi_{mk_{(1)}})} \\ &T_{k_{(1)}k_{(1)}'}^{j}(\alpha) \\ &\quad = \sum_p H_p^{(1)}(k_{uj}\rho_{k_{(1)}k_{(1)}'}) e^{-ip(\alpha + \phi_{k_{(1)}k_{(1)}'} - (\pi/2))}\, W(p) \\ &\tilde{\boldsymbol{\beta}}_{k_{(1)}'n}^{aj}(\alpha) \\ &\quad = \int_{S_n'} dS'\, \boldsymbol{J}_n(\boldsymbol{r}') e^{ik_{uj}\rho_{k_{(1)}'^n}\cos(\alpha + \phi_{k_{(1)}'^n})} \\ &\tilde{\beta}_{k_{(1)}'n}^{qj}(\alpha) \\ &\quad = \int_{S_n'} dS'\, \boldsymbol{J}_n(\boldsymbol{r}') e^{ik_{uj}\rho_{k_{(1)}'^n}\cos(\alpha + \phi_{k_{(1)}'^n})} \end{aligned}$$

ρ_{ji} and ϕ_{ji} are the amplitude and phase angle, respectively, of the vector $\boldsymbol{r}_i - \boldsymbol{r}_j$, and $W(p)$ is a window function. Here, $\boldsymbol{r}_{k_{(1)}}$ and $\boldsymbol{r}_{k'_{(1)}}$ are the centers of the $k_{(1)}$th and $k'_{(1)}$th groups at the finest level (first level), which currents $\boldsymbol{J}_m(\boldsymbol{r})$ and $\boldsymbol{J}_n(\boldsymbol{r}')$ belong to, respectively.

The matrix–vector multiplication used in each iteration can be written as

$$\begin{aligned}\sum_{n=1}^{N} Z_{mn}I_n = &\sum_{k'_1\in B_{k_1}}\sum_{n\in G_{k'_1}} Z_{mn}I_n \\ &+\sum_j w_j^u g^a(k_{uj})\,\frac{1}{2\pi}\int_0^{2\pi} d\alpha\;\tilde{\beta}^{aj}_{mk_{(1)}}(\alpha) \\ &\cdot\sum_{k'_1\notin B_{k_1}} T^j_{k_{(1)}k'_{(1)}}(\alpha)\sum_{n\in G_{k'_1}}\tilde{\boldsymbol{\beta}}^{aj}_{k'_{(1)}n}(\alpha)I_n \\ &-\sum_j w_j^u g^q(k_{uj})\,\frac{1}{2\pi}\int_0^{2\pi} d\alpha\;\tilde{\beta}^{qj}_{mk_{(1)}}(\alpha) \\ &\cdot\sum_{k'_1\notin B_{k_1}} T^j_{k_{(1)}k'_{(1)}}(\alpha)\sum_{n\in G_{k'_1}}\tilde{\beta}^{qj}_{k'_{(1)}n}(\alpha)I_n\end{aligned} \tag{16}$$

for $m \in G_{k_{(1)}}$, where $G_{k_{(1)}}$ denotes all elements in the $k_{(1)}$th group, and $B_{k_{(1)}}$ denotes all groups nearby of the $k_{(1)}$th group (including itself). The first term in (16) is the contribution from the nearby groups, and the last two terms represent contributions from well-separated groups. The physical interpretation of the last two terms in (16) is that different scattering centers within a group are first translated into a single center (aggregation). Hence, the number of the scattering centers is reduced. Similarly, for each group, the field scattered by all the other nonnearby group centers can be first received by the group center (translation), and then redistributed to the subscatterers belonging to the group (disaggregation).

If we choose each center of the group as a single scatterer and apply the fast multipole idea from the finest level to the coarsest level, then TSM-FMA is constructed. TSM-FMA for matrix–vector multiplication is broken down into two sweeps [5], [6], [20]. The first sweep consists of constructing an outgoing plane-wave expansion for each nonempty group at all levels. The second sweep consists of constructing incoming plane-wave expansions by combining contributions from well-separated groups at all levels. Below, we illustrate these techniques in applying TSM-FMA to the second term of (16). The third term of (16) can be handled similarly. During the first sweep, the number of outgoing plane-wave expansion should increase as plane-wave spectra are aggregated from a finer level to a coarser level. The expansions for the coarser level can be obtained from the finer level by interpolation. Let $\boldsymbol{r}_{k_{(l+1)}}$ and $\boldsymbol{r}_{k_{(l)}}$ be the group centers at level $l+1$ and l, respectively, then the outgoing wave for the coarser level $l+1$ is described in terms of the samples [5]

$$\tilde{\boldsymbol{b}}^{aj}_{k'_{(l+1)}}(\alpha_{\nu'}) = \tilde{\beta}^{aj}_{k'_{(l+1)}k'_{(l)}}(\alpha_{\nu'})\sum_{\nu\in U_{\nu'}} a_{\nu'\nu}\tilde{\boldsymbol{b}}^{aj}_{k'_{(l)}}(\alpha_\nu) \tag{17}$$

where

$$\tilde{\beta}^{aj}_{k'_{(l+1)}k'_{(l)}}(\alpha_{\nu'}) = e^{ik_{uj}\rho_{k'_{(l+1)}k'_{(l)}}\cos(\alpha_{\nu'}+\phi_{k'_{(l+1)}k'_{(l)}})}$$

$$\tilde{\boldsymbol{b}}_{k'_{(1)}}(\alpha) = \sum_{n\in G_{k'_1}}\tilde{\boldsymbol{\beta}}^{aj}_{k'_{(1)}n}(\alpha)I_n$$

$a_{\nu'\nu}$ are the interpolation coefficients, and $U_{\nu'}$ is a set of points in the neighborhood of point ν'. During the second sweep, the local expansions for smaller groups include the contribution from the parent group (disaggregation), and from the well-separated groups at the same level, but not the well-separated groups at the parent level (translation). A translation can be calculated by the T factor in (16) with FFT and interpolation because the sampling points are kept the same. At the coarsest level, only translations need to be calculated because contributions are from well-separated groups.

The disaggregation also faces the problem of the different number of the sampling points of α. If the local plane-wave expansions received by a group center $k_{(l+1)}$ at level $l+1$ is $\tilde{\boldsymbol{S}}^{aj}_{k_{(l+1)}}(\alpha)$, then its contribution to a child group center $k_{(l)}$ at level l can be written as [5]

$$\begin{aligned}[\boldsymbol{S}^{aj}_{k_{(l)}}]_n &= \frac{1}{2\pi}\int_0^{2\pi} d\alpha\; e^{in(\alpha-(\pi/2))}\tilde{\beta}^{aj}_{k_{(l)}k_{(l+1)}}(\alpha)\tilde{\boldsymbol{S}}^{aj}_{k_{(l+1)}}(\alpha) \\ &= \sum_{\nu'=1}^{Q_{l+1}} w^\alpha_{\nu'}\, e^{in(\alpha_{\nu'}-(\pi/2))}\tilde{\beta}^{aj}_{k_{(l)}k_{(l+1)}}(\alpha_{\nu'})\tilde{\boldsymbol{S}}^{aj}_{k_{(l+1)}}(\alpha_{\nu'})\end{aligned} \tag{18}$$

where $w^\alpha_{\nu'}$ is the weighting function. Substituting the interpolation expression for $e^{in(\alpha_{\nu'}-(\pi/2))}$ into (18), and exchanging the order of the summations lead to

$$\begin{aligned}[\boldsymbol{S}^{aj}_{k_{(l)}}]_n = &\sum_{\nu=1}^{Q_l} w^\alpha_\nu\, e^{in(\alpha_\nu-(\pi/2))} \\ &\cdot\sum_{\nu'}\frac{w^\alpha_{\nu'}}{w^\alpha_\nu}\,a_{\nu'\nu}\tilde{\beta}^{aj}_{k_{(l)}k_{(l+1)}}(\alpha_{\nu'})\tilde{\boldsymbol{S}}^{aj}_{k_{(l+1)}}(\alpha_{\nu'}).\end{aligned} \tag{19}$$

It is obtained from (19)

$$\tilde{\boldsymbol{S}}^{aj}_{k_{(l)}}(\alpha_\nu) = \sum_{\nu'}\frac{w^\alpha_{\nu'}}{w^\alpha_\nu}\,a_{\nu'\nu}\tilde{\beta}^{aj}_{k_{(l)}k_{(l+1)}}(\alpha_{\nu'})\tilde{\boldsymbol{S}}^{aj}_{k_{(l+1)}}(\alpha_{\nu'}). \tag{20}$$

The above operation is called anterpolation [6], [8]. By using anterpolation, the problem of unequal sampling rates can be solved with $O(Q)$ floating-point operations, where Q is the number of sampling points. It is shown from (15) that there are decaying terms with respect to the distance between the group centers in aggregation and disaggregation. The group center shifting distances are the same from one level to another. Therefore, we can choose different

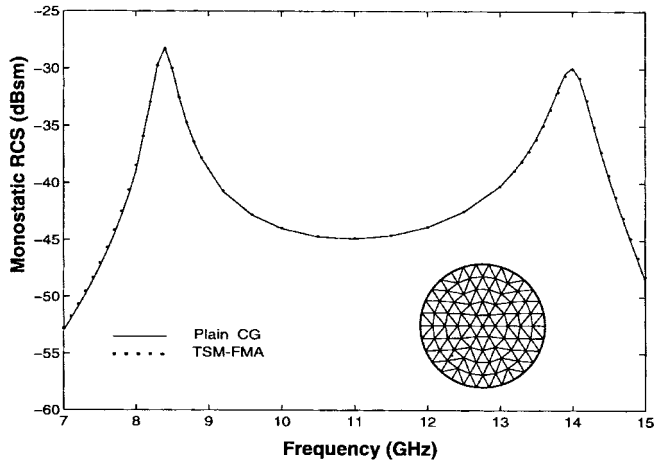

Fig. 3. Monostatic RCS versus frequency of a circular patch. Radius = 0.65 cm, $d = 0.07874$ cm, $\epsilon_r = 2.33$, $(\theta^i, \phi^i) = (60^\circ, 180^\circ)$, $\theta - \theta$ polarization.

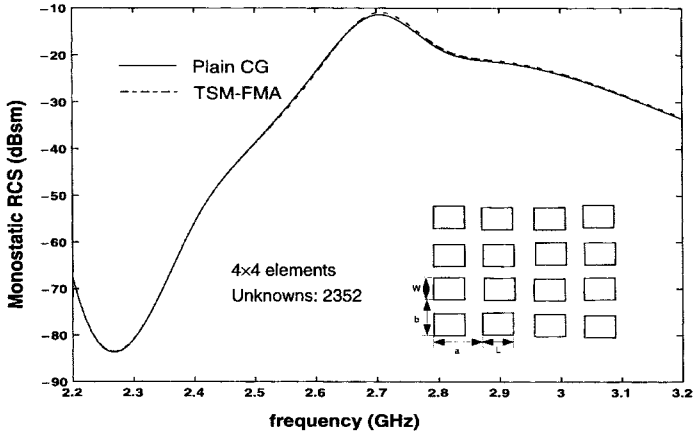

Fig. 4. Comparison of the monostatic RCS versus the frequency between TSM-FMA and plain CG method. 4×4 microstrip antenna array, $a = 8$ cm, $b = 8$ cm, $L = 3.66$ cm, $W = 2.60$ cm, $\epsilon_r = 2.17$, $d = 0.158$ cm, $(\theta^i, \phi^i) = (60^\circ, 45^\circ)$, $\theta - \theta$ polarization.

sets of integration points along the vertical branch cut at different levels to reduce the number of integration points. Similar interpolation and anterpolation techniques as described above can be used in aggregation and disaggregation, respectively.

At the finest level, the contribution from the nearby groups are calculated directly, and is represented by the first term on the right-hand side of (16). Green's functions used in this term are calculated directly with the numerical technique described in Section II-A. The terms g^p, $g^{\mathrm{TM},R}$, and g^{EM} appearing in the Dyadic Green's function are functions of radial distance ρ between observation and source points. In order to accelerate the calculation of the matrix elements within the nearby groups, precalculated tables of Green's functions versus distance between source and field points are constructed. These tables are stored as a database and interpolated repeatedly when accessed. The same Green's function tables are valid for any new conductor shape as long as the layer parameters remain the same.

At each level, the number of plane-wave expansions of a group is proportional to the dimension of the group. The number of unknowns is proportional to the area of the patch. Therefore, if the complexity analysis similar to [5] is performed, for the dense structures, the CPU time and memory requirement are $O(N)$, where N is the number of unknowns. For sparse structures, only nonempty groups are stored and calculated, The CPU time and memory requirement scale as $O(N \log N)$.

IV. Numerical Results

To validate TSM-FMA and to show its versatility in dealing with arbitrary shaped patches, the monostatic RCS of a circular patch is calculated as a function of the frequency by using TSM-FMA. The same result is computed using the plain CG method, with results shown in Fig. 3. The agreement between these two methods is excellent. The results also agree very well with the calculated result obtained by Aberle using entire domain basis functions, shown in [21]. Fig. 4 shows the

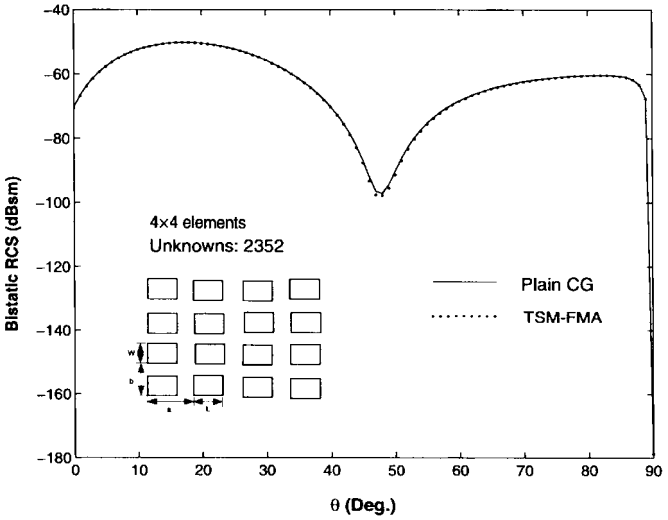

Fig. 5. Comparison of the bistatic RCS between TSM-FMA and plain CG method. 4×4 microstrip antenna array, $a = 6$ cm, $b = 6$ cm, $L = 3.66$ cm, $W = 2.60$ cm, $\epsilon_r = 2.17$, $d = 0.158$ cm, $(\theta^i, \phi^i) = (60^\circ, 45^\circ)$, $\theta - \theta$ polarization, frequency = 2.2 GHz.

monostatic RCS of a 4×4 microstrip array with rectangular patch elements versus frequency. Fig. 5 shows the bistatic RCS of a 4×4 element array. All the results are in excellent agreement with those obtained using plain CG.

Fig. 6 shows the comparison of the CPU time per iteration and the CPU time used for matrix filling between the TSM-FMA and the plain CG method. TSM-FMA is more efficient even for a small number of unknowns. Fig. 7 shows the memory requirements, the CPU time for matrix filling, and CPU time per iteration for TSM-FMA as a function of the number of unknowns. The structures calculated in Figs. 6 and 7 are a square element array with the parameters shown in Fig. 4, except that the number of elements is changed to yield different number of unknowns. Because the structures are not very sparse, the CPU time per iteration and memory requirements are almost linear with respect to the number of unknowns.

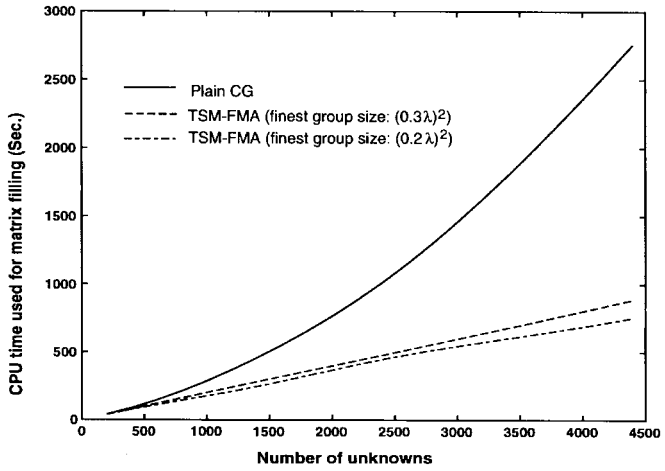

(a)

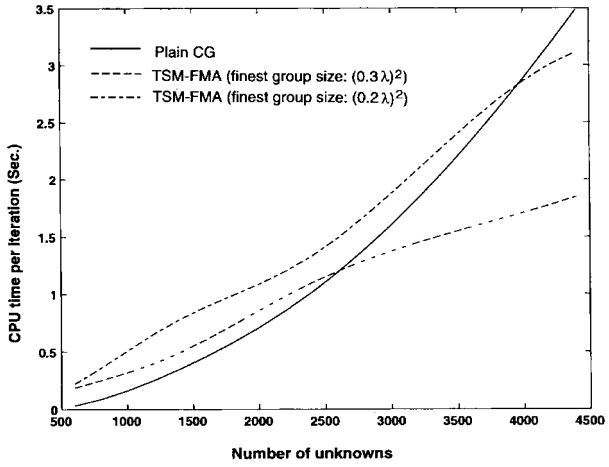

(b)

Fig. 6. Comparison of the CPU time for matrix filling and (a) the CPU time per iteration versus (b) the number of unknowns between TSM-FMA and plain CG method.

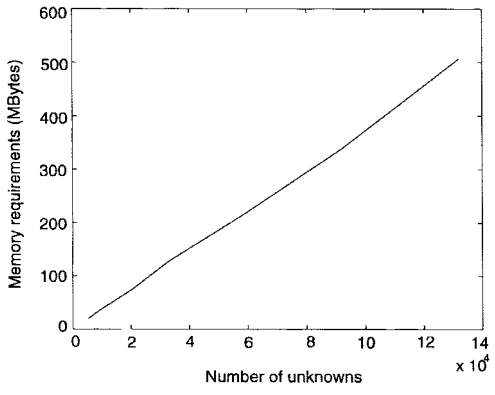

(a)

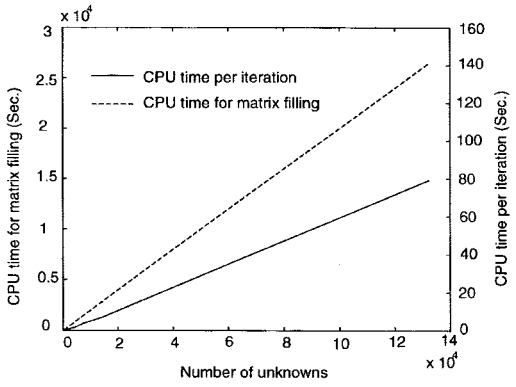

(b)

Fig. 7. Memory requirements. (a) CPU time per iteration and (b) CPU time for matrix filling as functions of number of unknowns for TSM-FMA.

Fig. 8 shows the bistatic RCS for a 30 × 30 element microstrip array with 130 000 unknowns. Only 507.6 Mbyte memory is needed and the CPU time per iteration is 79.23 s using one processor of an SGI Power Challenge machine (R8000). It is clear that TSM-FMA needs much less memory and takes much less CPU time compared to a standard matrix solver.

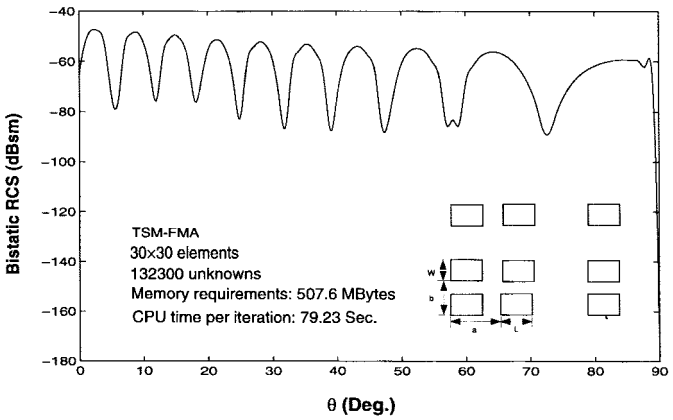

Fig. 8. Bistatic RCS for a 30 × 30 microstrip antenna array. $a = 6$ cm, $b = 6$ cm, $L = 3.66$ cm, $W = 2.6$ cm, $\epsilon_r = 2.17, d = 0.158$ cm, frequency = 2.2 GHz, $(\theta^i, \phi^i) = (60°, 45°)$, $\theta - \theta$ polarization.

V. Conclusions

This paper has introduced the TSM-FMA which permits the efficient full-wave analysis of large microstrip structures. When compared to the plain CG method, TSM-FMA reduces the CPU time to $O(N)$ for dense structures and $O(N \log N)$ for sparse structures from $O(N^2)$ for the plain CG method. The memory requirement for TSM-FMA is also $O(N)$ for dense structures and $O(N \log N)$ for sparse structures. The computational complexity for CG-FFT is $O(N)$ for the memory requirement and $O(N \log N)$ for the CPU time when the structure is densely packed. However, when the structure is sparse (e.g., where microstrip lines lie on top of the substrate with much empty space in between), CG-FFT is inefficient because the empty space has to be padded with zeros in a 2-D-FFT. For instance, for the case of a loop of microwave integrated-circuit waveguide, the computational complexity for CG-FFT is $O(N^2)$ and $O(N^2 \log N)$ for the memory requirement and CPU time, respectively (not better than a plain CG).

For regular grid geometries (e.g., rectilinear meshes with dense structures), which are well suited for a 2-D-FFT, CG-

FFT is in fact more efficient because of the efficiency of the FFT algorithm which has been around for several decades. However, an algorithm developed for a regular mesh is not easily adaptable to irregular meshes or arbitrarily shaped patches. TSM-FMA uses the fast multipole algorithm concept. At this point, the proportionality constant in front of the aforementioned computational complexity analysis if still large compared to FFT. However, TSM-FMA holds high promise as an efficient algorithm for a patch of arbitrary shape and arbitrary packing density. It even allows an uneven gridding of the geometry.

REFERENCES

[1] T. K. Sakar, E. Arvas, and S. S. Rao, "Application of FFT and conjugate gradient method for the solution of electromagnetic radiation from electrically large and small conducting bodies," *IEEE Trans. Antennas Propagat.*, vol. AP-34, pp. 635–640, May 1986.

[2] Y. Zhuang, K. L. Wu, C. Wu, and J. Litva, "A combined full-wave CG-FFT method for rigorous analysis of large microstrip antenna arrays," *IEEE Trans. Antennas Propagat.*, vol. 44, pp. 102–109, Jan. 1996.

[3] V. Jandhyala, E. Michielssen, and R. Mittra, "Multipole-accelerated capacitance computation for 3-D structures in a stratified dielectric medium using a closed form Green's function," (Special issue on Microwave Packages and Interconnects), *Int. J. Microwave Millimeter-Wave Comput.-Aided Eng.*, vol. 5, pp. 68–78, May 1995.

[4] L. Gurel and M. I. Aksun, "Electromagnetic scattering solution of conducting strips in layered media using the fast multipole method," *IEEE Microwave Guided Wave Lett.*, vol. 6, pp. 277–279, Aug 1996.

[5] C. C. Lu and W. C. Chew, "A multilevel algorithm for solving a boundary integral equation of wave scattering," *Microwave Opt. Technol. Lett.*, vol. 7, no. 10, pp. 456–470, July 1994.

[6] J. M. Song and W. C. Chew, "Multilevel fast-multipole algorithm for solving combined field integral equations of electromagnetic scattering," *Microwave Opt. Technol. Lett.*, vol. 10, no. 1, pp. 14–19, Sept. 1995.

[7] V. Rokhlin, "Rapid solution of integral equations of scattering theory in two dimensions," *J. Comput. Phys*, vol. 36, no. 2, pp. 414–439, 1990.

[8] A. Brandt, "Multilevel computations of integral transforms and particle interactions with oscillatory kernels," *Comput. Phys. Commun.*, vol. 65, pp. 24–38, 1991.

[9] W. C. Chew and C. C. Lu, "A fast algorithm to compute the wave-scattering solution of a large strip," *Computational Phys.*, vol. 107, no. 2, pp. 378–387, Aug. 1993.

[10] C. C. Lu and W. C. Chew, "Electromagnetic scattering of finite strip array on a dielectric slab," *IEEE Trans. Microwave Theory Tech.*, vol. 41, pp. 97–100, Jan. 1993.

[11] E. Michielssen and W. C. Chew, "The fast steepest descent path algorithm for analyzing scattering from two-dimensional objects," *Radio Sci.*, vol. 31, no. 5, pp. 1215–1224, Sept.-Oct. 1996.

[12] V. Jandhyala, E. Michielssen, B. Shanker, and W. C. Chew, "A combined steepest descent–fast multipole algorithm for the fast analysis of three-dimensional scattering by rough surfaces," Center Computational Electromagnetics Res. Rep. CCEM 3-97, Mar. 31, 1997.

[13] K. A. Michalski and D. Zheng, "Electromagnetic scattering and radiation by surfaces of arbitrary shape in layered media, part I: Theory," *IEEE Trans. Antennas Propagat.*, vol. 38, pp. 335–344, Mar. 1990.

[14] M. J. Tsai, F. D. Flaviis, O. Fordham, and N. G. Alexopoulos, "Modeling planar arbitrarily shaped microstrip elements in multilayered media," *IEEE Trans. Microwave Theory Tech.*, vol. 45, pp. 330–337, Mar. 1997.

[15] W. C. Chew, *Waves and Fields in Inhomogeneous Media*. New York: Van Nostrand, 1990.

[16] J. A. Kong, *Theory of Electromagnetic Waves*. New York: Wiley, 1975.

[17] S. M. Rao, D. R. Wilton, and A. W. Glisson, "Electromagnetic scattering by surfaces of arbitrary shape," *IEEE Trans. Antennas Propagat.*, vol. AP-30, pp. 407–418, May 1982.

[18] P. B. Katehi and N. G. Alexopoulos, "Frequency-dependent characteristics of microstrip discontinuities in millimeter-wave integrated circuits," *IEEE Trans. Microwave Theory Tech.*, vol. MTT-33, pp. 1029–1035, Oct. 1985.

[19] D. M. Pozar, "Radiation and scattering from a microstrip patch on a uniaxial substrate," *IEEE Trans. Antennas Propagat.*, vol. AP-35, pp. 613–621, June 1987.

[20] C. R. Anderson, "An implementation of the fast multipole method without multipole," *SIAM J. Sci. Stat. Comput.*, vol. 13, no. 4, pp. 923–947, July 1992.

[21] D. G. Shively *et al.*, "Scattering from microstrip patch antennas using subdomain basis functions," *Electromagnetics*, vol. 14, pp. 1–18, 1994.

Jun-Sheng Zhao was born in Shandong Province, China, on April 17, 1966. He received the B.S. degree from Shandong University, Jinan, China, in 1985, the M. Eng. degree from the Second Academy of the Ministry of the Astronautics Industry of China (now China Aerospace Industry Corporation), Beijing, China, in 1988, and the Ph.D. degree from Tsinghua University, Beijing, China, in 1995, all in electrical engineering.

From July 1988 to February 1992, and from July 1995 to January 1996, he worked at the Second Academy of the Ministry of the Astronautics Industry of China. Since February 1996, he has been a Visiting Post-Doctoral Research Associate at the Center for Computational Electromagnetics, University of Illinois at Urbana-Champaign. His research interests include fast algorithms for computational electromagnetics, microwave integrated circuits, and ferrite devices.

Weng Cho Chew (S'79–M'80–SM'86–F'93) was born on June 9, 1953, in Malaysia. He received the B.S. degree, both the M.S. and Engineer's degrees, and the Ph.D. degree from the Massachusetts Institute of Technology, Cambridge, in 1976, 1978, and 1980, respectively, all in electrical engineering.

From 1981 to 1985, he was with Schlumberger-Doll Research, Ridgefield, CT, where he was a Program Leader and a Department Manager. From 1985 to 1990, he was an Associate Professor with the University of Illinois at Urbana-Champaign, and is currently a Professor teaching graduate courses in waves and fields in inhomogeneous media, and theory of microwave and optical waveguides, and supervising a graduate research program. From 1989 to 1993, he was the Associate Director of the Advanced Construction Technology Center, University of Illinois at Urbana-Champaign, where he is currently the Director of the Center for Computational Electromagnetics and the Electromagnetics Laboratory. His name is listed in the university's *List of Excellent Instructors*. He has authored *Waves and Fields in Inhomogeneous Media* (New York: Van Nostrand, 1990), published over 175 scientific journal articles, and presented over 200 conference papers. His recent research interest has been in the area of wave propagation, scattering, inverse scattering, and fast algorithms related to scattering, inhomogeneous media for geophysical subsurface sensing, and nondestructive testing applications. He has also previously analyzed electrochemical effects and dielectric properties of composite materials, microwave and optical waveguides, and microstrip antennas. He is an associate editor of *Journal of Electromagnetic Waves and Applications*, and *Microwave Optical Technology Letters*. He was also an associate editor with the *International Journal of Imaging Systems and Technology*, and has been a guest editor of *Radio Science*, *International Journal of Imaging Systems and Technology*, and *Electromagnetics*.

Dr. Chew is a member of Eta Kappa Nu, Tau Beta Pi, URSI Commissions B and F, and the Society of Exploration Geophysics. He has been an Ad Com member of the IEEE Geoscience and Remote Sensing Society, and is currently an associate editor of the IEEE TRANSACTIONS ON GEOSCIENCE AND REMOTE SENSING, He was a National Science Foundation (NSF) Presidential Young Investigator in 1986.

Cai-Cheng Lu (S'95–M'95) was born in Hubei, China. He received the B.S. and M.S. degrees in electrical engineering from Beijing University of Aeronautics and Astronautics, Beijing, China, in 1983 and 1986, respectively, and the Ph.D. degree in electrical engineering from the University of Illinois at Urbana-Champaign, in 1995.

From May 1996 to May 1997, he worked in the Center for Computational Electromagnetics, University of Illinois at Urbana-Champaign, first as a Post-Doctoral Research Associate, and then as a Research Scientist. He is currently with Demaco, Inc., Champaign, IL. He co-authored the fast Illinois solver code (FISC), which uses the MLFMA to solve large problems in electromagnetic interaction with complex structures. His interests include fast algorithms for computational electromagnetics, electromagnetic-wave scattering and inverse scattering, SAR image simulation, and processing.

Dr. Lu is a member of Phi Kappa Phi.

Eric Michielssen (M'95) received the M.S. degree in electrical engineering from Katholieke Universiteit Leuven (KUL), Leuven, Belgium, 1987, and the Ph.D. degree from the University of Illinois at Urbana-Champaign, in 1992.

From 1987 to 1988, he was a Research Assistant in the Microwaves and Lasers Laboratory, KUL. In 1988, he was appointed Belgian American Educational Foundation Fellow. In 1992, he joined the Faculty of the Department of Electrical and Computer Engineering at the University of Illinois at Urbana-Champaign as a Visiting Assistant Professor, was appointed Assistant Professor of electrical and computer engineering, and is also the Associate Director of its Center for Computational Electromagnetics. His research interests include all aspects of computational electromagnetics, with a focus on fast multilevel algorithms, the application of combinatorial stochastic optimization techniques to the design of electromagnetic and optical components, and computational photonics. He serves as associate editor for *Radio Science* and as the technical chair for the 13th Annual Review of Computational Electromagnetics (ACES'97, Monterey, CA).

Dr. Michielssen was the recipient of the 1995 National Science Foundation (NSF) Career Award.

Jiming Song (S'92–M'95) received the B.S. and M.S. degrees in physics from Nanjing University, Nanjing, China, in 1983 and 1988, respectively, and Ph.D. degree in electrical engineering from Michigan State University, East Lansing, in 1993.

From 1983 to 1985, he worked in the Department of Microwave Engineering, Beijing Broadcasting College, Beijing, China. From 1993 to 1995, he worked as a Post-Doctoral Research Associate at the University of Illinois at Urbana-Champaign. He is currently a Research Scientist and Visiting Assistant Professor at the University of Illinois at Urbana-Champaign and a Research Scientist at Demaco Inc., Champaign, IL. His research has dealt with wave scattering using fast algorithms, wave interaction with inhomogeneous media, transient electromagnetic field, and high-Tc superconductive electronics.

Dr. Song is a member of Phi Kappa Phi. He was the recipient of the 1992 Outstanding Academic Award given by the College of Engineering, Michigan State University.